INVESTIGATION OF THE INFLUENCE OF FIBRE SIZINGS ON THE CRACK BRIDGING BEHAVIOUR OF GLASS FIBRE COMPOSITES

S. Feih, B.F. Sørensen

Materials Research Department, Risø National Laboratory, Roskilde, Denmark

ABSTRACT

The influence of different fibre sizings on the strength and fracture toughness of composites was studied by investigating the characteristics of fibre cross-over bridging in DCB specimens loaded with pure bending moments. Bridging laws were obtained by simultaneous measurements of the crack growth resistance and the end opening of the notch. For a given composite system, the parameters of the bridging law depend on the interfacial properties of the fibre/ matrix interphase. The crack initiation value correlates with the composite transverse strength, while fracture toughness determines crack growth and damage development. Micromechanical investigations by environmental scanning electron microscopy visualise the differences in bridging behaviour. The bridging laws were taken to be material laws and were implemented in a numerical model to study aspects of crack development.

1. INTRODUCTION

For glass fibre composites, the interfacial properties are controlled by the sizing, which provides a physico-chemical link between the glass surface and the matrix system. The sizing, which has a complex composition, is applied to the glass fibres during manufacture and also protects the fibre surface from damage and binds fibres together for ease of processing. For the same matrix system, a change of sizing results in changes of the interfacial properties, thereby influencing the overall mechanical properties, such as strength and fracture toughness, of the composite material. A thorough understanding of the interfacial properties can therefore help to tailor composites for specific applications. However, it needs to be considered that optimising the strength of the composite can lead to a reduction in the fracture toughness and vice versa.

2. PRINCIPLE OF MEASURING BRIDGING LAWS

The approach for the measurements of bridging laws is based on the application of the path independent J integral [1], and has been used recently to determine the bridging characteristics of unidirectional carbon fibre/ epoxy composites [2] and glass fibre composites [3]. A symmetric DCB specimen is loaded with pure bending moments M (Fig. 1). This specimen is one of the few practical specimen geometries for which the global J integral (i.e. the integral evaluated around the external boundaries of the specimen) can be determined analytically, even though large scale bridging occurs [1, 4]:

$$J = 12(1-\nu_{13}\nu_{31})\frac{M^2}{b^2 H^3 E_{11}} \tag{1}$$

E_{11} is the Young's modulus referring to the material directions, ν_{13} and ν_{31} are the major and minor Poisson's ratio, b is the width and H the beam height. The material consists of unidirectional composites with fibres aligned in x_1-direction.

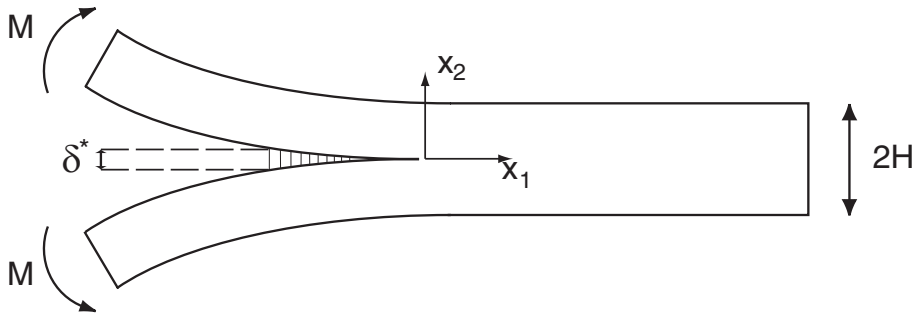

"**Fig. 1.** DCB specimen with pure bending moment"

The specimen is assumed to have a crack with bridging fibres across the crack faces near the tip. The closure stress σ (x_2-direction) can be assumed to depend only on the local crack opening δ. The bridging law $\sigma = \sigma(\delta)$ is then taken as identical at each point along the bridging zone. Since fibres will fail when loaded sufficiently, we assume the existence of a characteristic crack opening δ_0, beyond which the closure traction vanishes. Shrinking the path of the J integral to the crack faces and around the crack tip [4] gives

$$J_{\mathrm{R}} = \int_0^{\delta^*} \sigma(\delta) d\delta + J_{\mathrm{tip}} \,, \tag{2}$$

where J_{tip} is the J integral evaluated around the crack tip (during cracking J_{tip} is equal to the fracture energy of the tip, J_0). The integral is the energy dissipation in the bridging zone, and δ^* is the end-opening of the bridging zone at the notch root. The bridging law can be determined by differentiating Eq. (2) [4].

$$\sigma(\delta^*) = \frac{\partial J_{\mathrm{R}}}{\partial \delta^*} \tag{3}$$

Thus, by recording J_R and the end opening of the bridging zone δ^*, the bridging law can be determined. In this approach, the bridging zone is modelled as a discrete mechanism on its own. Contrary to the classical R-curves (fracture resistance as a function of crack length), the bridging law can be considered a material property and does not depend on specimen size [4].

3. EXPERIMENTAL METHODS

We investigated two commercial E-glass fibre systems with the same fibre diameters (~17μm ± 2μm), but different silane-based sizings. Sizing A is described as multi-purpose compatible, while sizing B is epoxy compatible. A detailed chemical analysis of the two fibre sizings, which clearly show differences regarding the surface groups, can be found in [3] and [5]. The two resin types consist of a bisphenol A-based epoxy resin and an orthophthalic polyester resin. An in-house developed resin transfer moulding technique was applied for the composite manufacture. The epoxy resin was cured at 120°C for six hours, and the polyester resin was cured at 50°C for 24 hours. The nominal fibre volume fraction was 55% for both systems.

The specimen width b was 5 mm with a beam height of H=8 mm (Fig. 1). The length of the specimen was 145 mm. The notch, cut with a 0.7mm wide diamond saw for a length of 36 mm, was parallel to the fibre direction and perpendicular to the plane of the plate. The subsequent crack growth was therefore intralaminar. At least 5 specimens of each fibre/ matrix type were tested. Extensometers were mounted at both faces of the specimen just at the end of the notch to record δ^* as a function of the applied bending moment. The crosshead

displacement was kept at 2 mm/min, which corresponds to 0.15mm/min for the end opening rate $d\delta^*/dt$ (t denotes time). Smaller DCB specimens (H=4 mm, b=5 mm) were loaded in a similar fashion within an environmental scanning electron microscope to study the details of crack development.

4. EXPERIMENTAL RESULTS

Crack initiation occurred at a certain applied moment, and the associated value of the crack growth resistance J_R is denoted J_0. With increasing applied moment, crack propagation took place. Fibre cross-over bridging developed in the zone between the notch and the crack tip. Fig. 2 shows the bridging fibre ligaments for the different systems at the end of the test. With increasing opening, the bridging fibres eventually broke at the end of the notch for the epoxy systems. This point represented the start of the steady-state cracking, where the bridging length remained approximately the same, and the bridging zone moved forward with the crack tip advancing into the specimen. The behaviour is nearly identical for the other epoxy composite. For the polyester resin systems, crack bridging was considerably more extensive, with the sizing B/ polyester system not indicating any fibre breakage at the notch. No steady-state fracture resistance was attained.

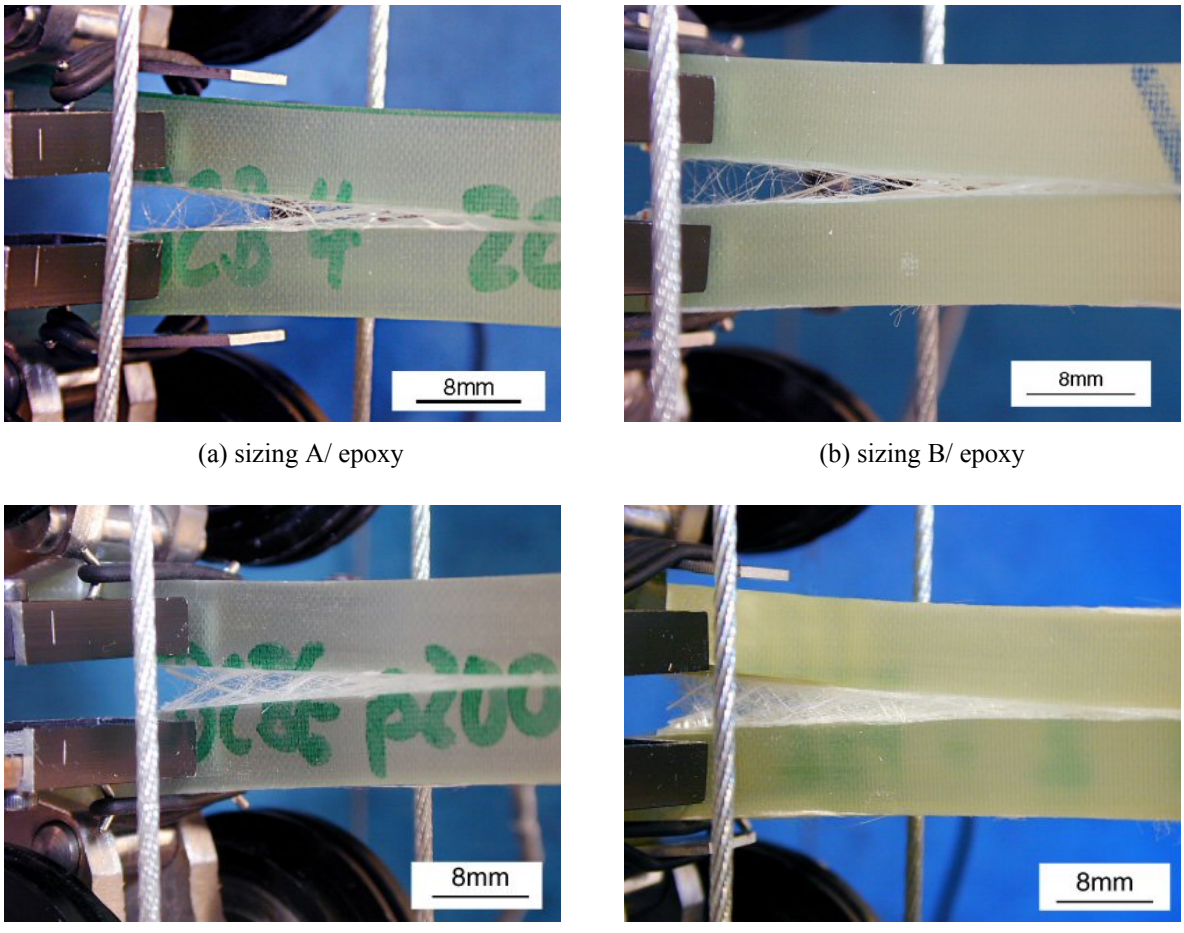

(a) sizing A/ epoxy

(b) sizing B/ epoxy

(c) sizing A/ polyester

(d) sizing B/ polyester

"**Fig. 2.** Crack bridging behaviour of composite systems"

Based on Fig. 2, significant differences were seen for the sizing B/ polyester composite system. These differences can be related to the bond between fibre and matrix as shown in

Fig. 3. Cracking takes place along and also into the fibres for the epoxy and the sizing A/ polyester systems (strong bond), while the sizing B/ polyester composite shows clear separation along the fibre/matrix interface, thereby indicating a weaker bond.

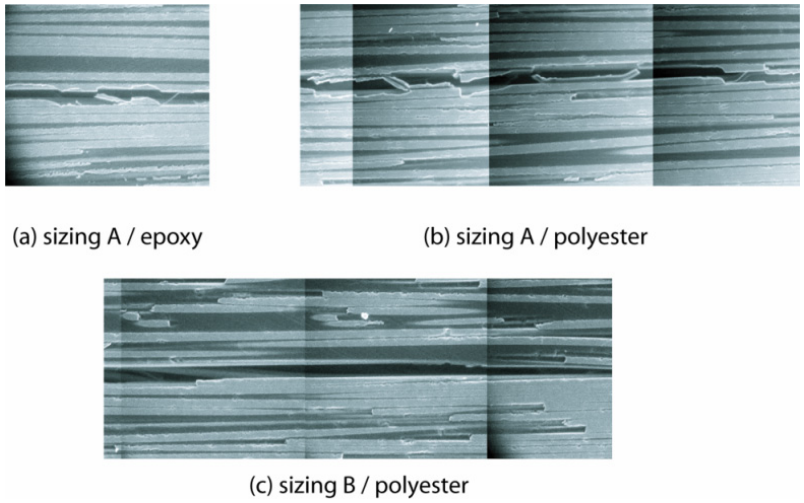

"**Fig. 3.** Difference in cracking due to fibre/matrix bond"

Fig. 4 visualises the resulting difference in crack bridging behaviour on the microscale. For the composite of sizing A/ epoxy, moderate fibre bridging was observed, where the ligament widths consisted mostly of around four fibres. These bridges tended to break at higher loads. For the composite with sizing B/ polyester, on the other hand, extensive bridging behaviour could be seen. With an advancing crack front, these bridging ligaments separated and multiple cracks developed. Not many fibres were found to fail.

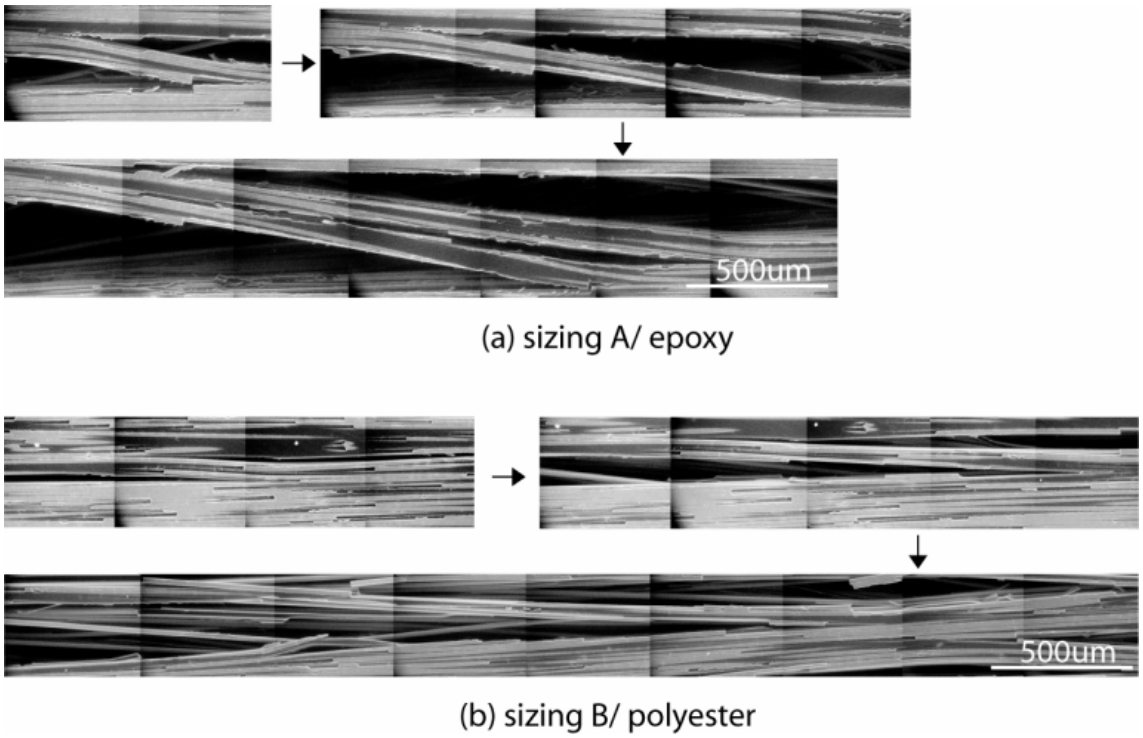

"**Fig. 4.** Micromechanical differences for strong (a) and weak (b) fibre/matrix bonding**"**

5. BRIDGING LAW PARAMETERS

We now proceed to analyse the experimental data. J_R is calculated according to Eq. (1). Assuming that the unidirectional composite is transversely isotropic, the following elastic composite data were applied for Eq. (1) as previously measured: $E_{11,\ epoxy}$= 41.5 GPa, E_{33}= 9.2 GPa, $E_{11,\ polyester}$ = 42 GPa, $E_{33,\ polyester}$= 10 GPa and ν_{13}=0.3 (assumption). The function

$$J_R\left(\delta^*\right) = J_0 + \Delta J_{ss}\left(\frac{\delta^*}{\delta_0}\right)^{1/2} \quad \text{for} \quad \delta^* \le \delta_0 \tag{4}$$

was found to fit all experimental data curves well. The experimental values for the bridging laws are given in Table 1. J_0 indicates the point of crack growth initiation and is equal to the fracture energy of the tip during crack growth, while ΔJ_{ss}, which is equal to (J_{ss}-J_0), is the increase in crack growth resistance, and J_{ss} is the steady-state fracture resistance. Sørensen and Jacobsen [2] found that the same function fits the data of carbon fibre composite systems.

"**Table 1.** Experimental bridging law parameters for the different fibre/matrix systems"

Composite system	J_0 [J/m^2]	ΔJ_{ss} [J/m^2]	δ_0 [mm]
sizing A/ epoxy	300±40	4000±1000	2.0±0.2
sizing B/ epoxy	355±15	3700±500	2.0±0.2
sizing A/ polyester	170±20	~3800	~5.5
sizing B/ polyester	115±45	>4100	>5.0

The crack initiation value J_0 can easily be determined during the experiment. The highest value of J_0=355 J/m^2 was observed for the sizing B/ epoxy system. The crack initiation value is significantly lower for the sizing B/ polyester system with J_0=115 J/m^2. J_0 can be related to the transverse composite strength, which is generally considered a sensitive macroscopic test to characterise the fibre/ matrix bond strength. Fig. 5 visualises the very satisfactory linear dependence of the crack initiation value J_0 on previous transverse strength measurements under 3-point bending (EN ISO 14125) [3]. Furthermore, the sensitivity of J_0 is of the same order of magnitude as the transverse bending strength (factor 3 for max/min difference).

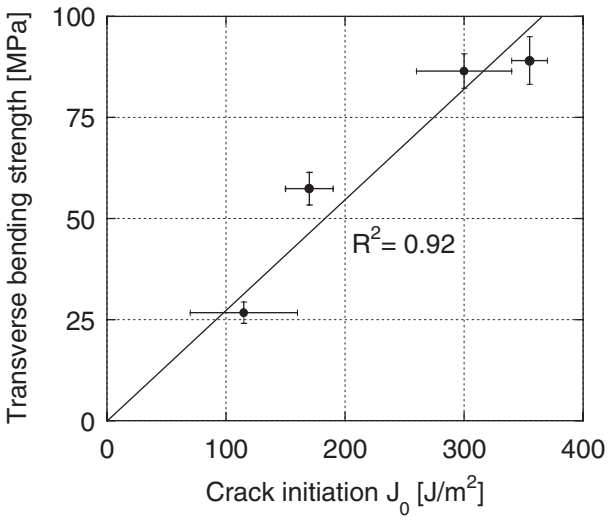

"**Fig. 5.** Correlation between transverse tensile strength and crack initiation energy"

The difference in crack bridging behaviour as seen in the previous figures is furthermore explained with this correlation: a relatively low amount of fibre bridging followed by fibre breaking is observed for a "strong" fibre/ matrix bond, which stresses the fibres, while multiple crack fronts and no fibre breakage are observed in the case of "weak" interfacial bonding due to easy debonding of fibre and matrix.

The end opening value at the onset of steady-state cracking δ_0 was determined to be 2 mm for the epoxy systems. For the sizing B/ polyester system, δ_0 and the steady-state fracture resistance could not be determined with the present specimen geometry, as the fibres continued to bridge the whole length of the crack after the maximum measurable end opening was obtained. Since no upper bound was found for ΔJ_{ss}, this bridging behaviour was termed 'infinite toughening'. The sizing A/ polyester system was found to lie in between the others in terms of end opening value δ_0 and increase in crack growth resistance ΔJ_{ss}.

Differentiating Eq. (5) results in the bridging law

$$\sigma\left(\delta^*\right) = \frac{\Delta J_{ss}}{2\left(\delta^* \delta_0\right)^{1/2}} . \tag{5}$$

The crack growth resistance and the resulting bridging laws for the different fibre systems are compared in Fig. 6. The bridging law in (b) can be considered a material property [6,7] and is in an accessible form for implementation in finite element codes.

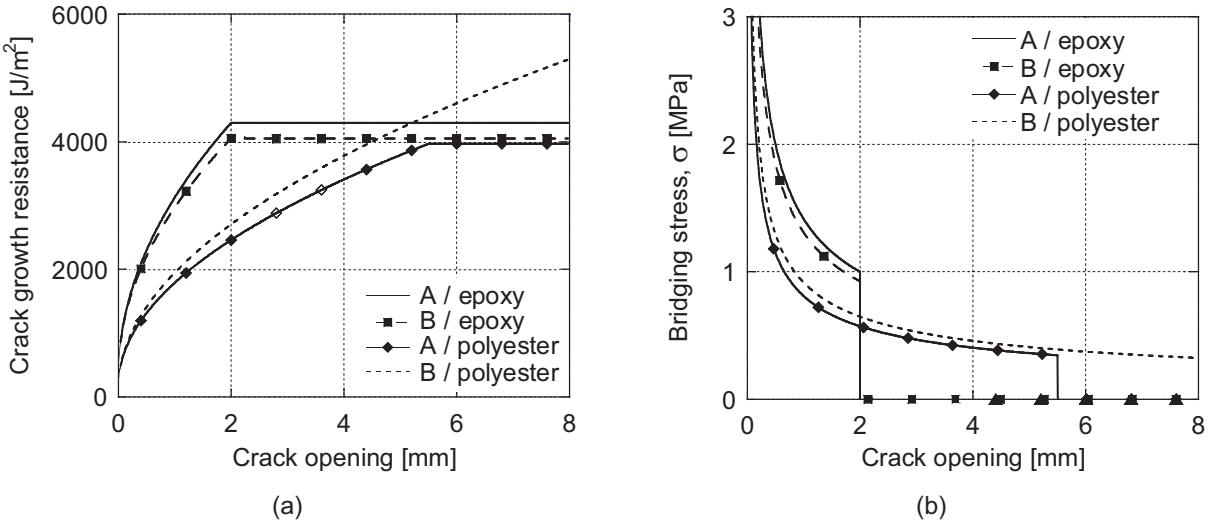

"**Fig. 6.** Comparison of (a) crack growth resistance and (b) resulting crack bridging laws"

6. NUMERICAL INVESTIGATION

Numerical simulations were undertaken with ABAQUS version 6.4. There are different possible methods of implementing cohesive laws within commercial finite element software. For the results presented here, ABAQUS' contact routine was adapted to account for the bridging stresses. The user subroutine UINTER was programmed to specify the stress-opening relations. Other possibilities include incorporation of spring elements or programming of user defined cohesive elements.

The modelling procedure is visualised in Fig. 7. Due to the symmetry conditions during mode I testing, only one beam of the DCB specimen needs to be modelled. The mesh consists of 8-noded plane strain solid CPE8 elements, which are suited to describe bending deformations.

The composite materials are assumed to be transversely isotropic with the material properties given in Section 5.

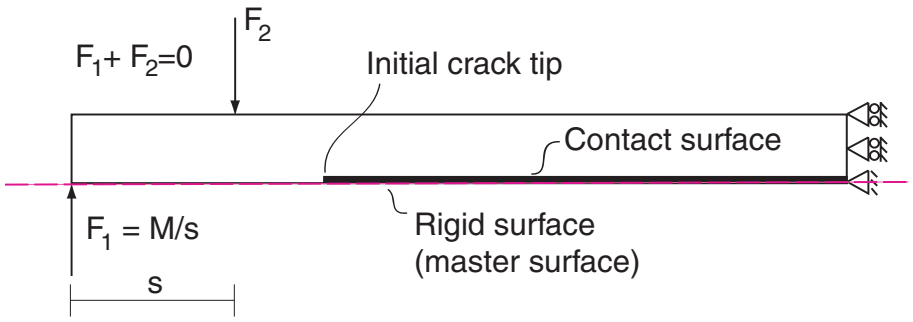

"**Fig. 7.** Problem statement and boundary conditions for DCB specimen under applied moments"

The contact problem is modelled as surface-based contact between a rigid surface (symmetry plane) and a deformable body (DCB beam). The moment application is undertaken with displacement control [6], which is preferred for analyses with possible decreasing structural forces due to material damage. The applied moment can be calculated from the reaction force F_1, and the J integral is subsequently determined from Eq. (1).

The fitted bridging law as derived in Eq. (5) exhibits a singularity in δ=0. Experimentally, the stress at δ=0 cannot be determined exactly, since following crack initiation the end opening has a finite value. A micromechanical model [7] predicts that crack initiation starts at a finite stress value at the interface, which is reached as deformation starts to take place. The experimental bridging law is adjusted to account for this finite stress level as shown in Fig. 8(a).

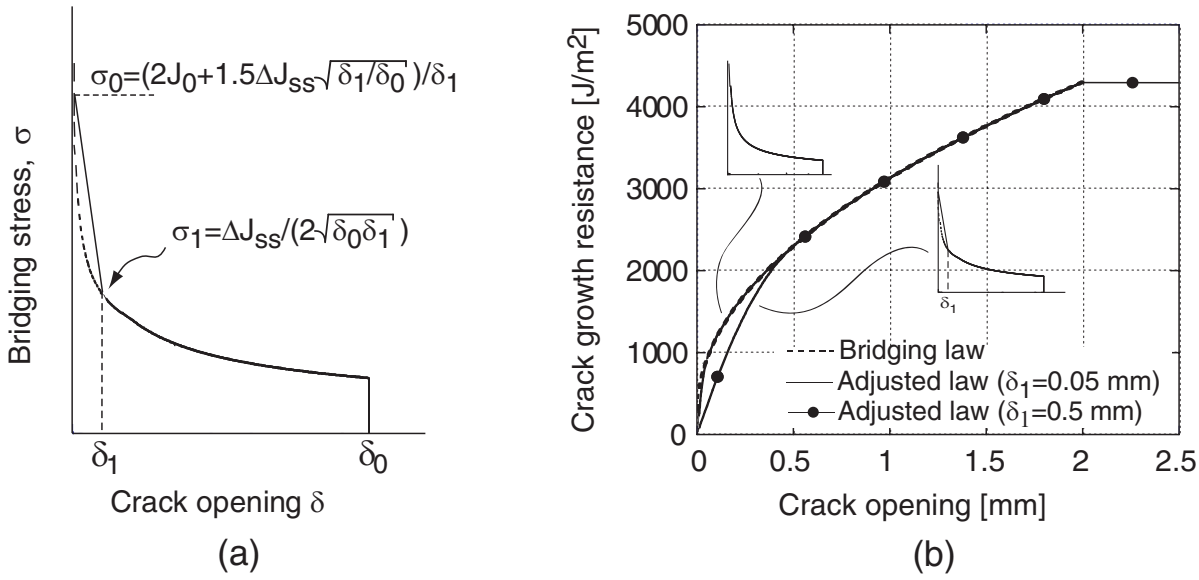

"**Fig. 8.** Adjustment of numerical bridging law (a) and resulting energy uptake (b)"

The stress value is found by requiring that the area under the linear softening law in the region $0 \leq \delta \leq \delta_1$ must equal the area of the general bridging law in this range and the crack initiation energy J_0. The value of J_0 needs to be added into the bridging law to ensure that the same final energy uptake is achieved with the numerical model (see Fig. 8(b)).

The following results focus on two of the composite systems: (1) sizing A/ epoxy and (2) sizing A/ polyester. The adjustments for the bridging law parameters are shown in Table 2. From a modelling point of view, the smallest possible value for δ_1 should be chosen to minimize differences due to the numerical adjustment. However, the finite stress value increases drastically with decreasing δ_1, thereby leading to numerical difficulties during the analysis. The value of δ_1=0.05 mm is small compared to the maximum crack opening δ_0 and leads to numerically stable runs for a reasonable level of mesh refinement.

"**Table 2.** Adjustment of bridging parameters"

System	J_0 [J/m^2]	ΔJ_{ss} [J/m^2]	δ_1 [mm]	δ_0 [mm]	σ_0 [MPa]
sizing A/epoxy	300	4000	0.05	2.0	31.0
sizing A/polyester	170	3800	0.05	5.5	17.7

The analyses were run with the modified Riks method in ABAQUS. The influence of mesh refinement was found to be negligible for the curves presented hereafter, although local stress differences exist at the advancing crack front due to the finite stress level of the bridging law at zero opening. Fig. 9 shows the resulting crack growth resistance predictions for both composite systems with one set of experimental data each.

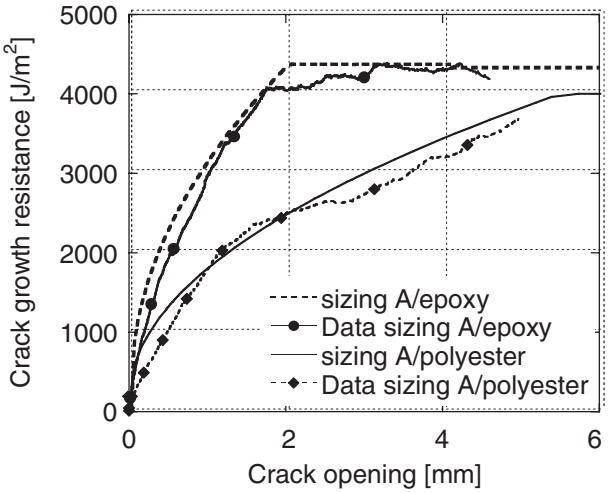

"**Fig. 9.** Comparison of numerical and experimental crack growth resistance"

Fig. 10 shows the distinct difference in the R-curves and crack opening versus crack extension curves for the two composite systems. The crack extension is nearly linear with crack growth resistance due to the shape of the bridging law. The same observation was made in previous work for carbon fibres using a different numerical approach [6]. It can furthermore be seen that the larger value of δ_0 in the bridging law for sizing A/ polyester (see

Fig. 6(b) and Table 1) leads to a significantly larger crack extension for a similar crack growth resistance.

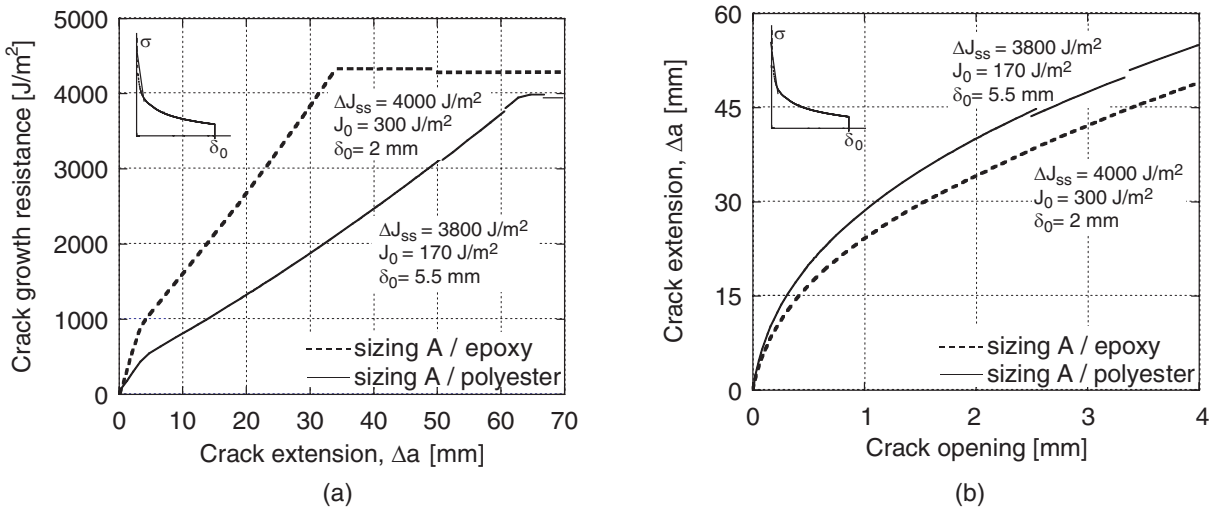

"**Fig. 10.** (a) Predicted R-curves as a function of crack extension and (b) crack opening vs. crack extension curve"

The numerical model can furthermore be applied to study the crack shape at specified loads or crack opening values. Fig. 11(a) shows the crack opening for a specified crack growth resistance of J_R=3100 J/m^2. As also seen in Fig. 9, the crack opening δ_0 is larger for a given crack growth resistance for sizing A/ poyester. The two corresponding unbridged profiles (same crack extension and applied moment) are also indicated in the figure. Of interest is the fact that the shape of the profile varies significantly in the crack tip vicinity. This difference is due to the continuously decreasing shape of the bridging law [8]. Fig. 11(b) shows how the crack shapes vary for two crack opening values of δ_0=0.3 mm and δ_0=1.2 mm. For the same crack opening, the crack extension for the sizing A / polyester system will be higher, and the crack growth resistance J_R will be significantly lower.

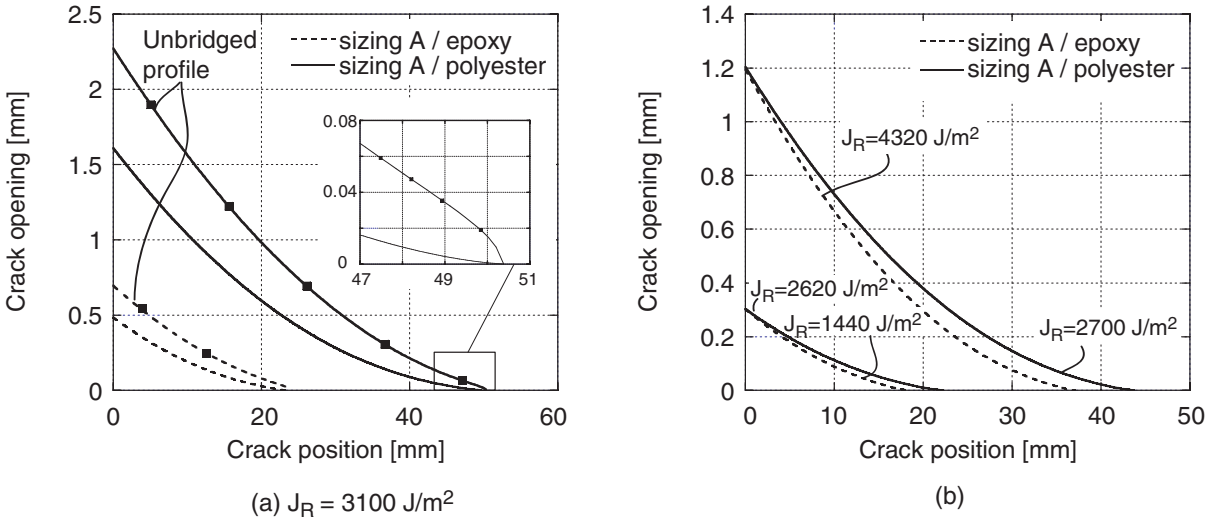

"**Fig. 11.** Comparison of crack opening shapes"

7. CONCLUSION

The current work emphasises that the characteristics of the interphase between fibre and matrix have a strong influence on the strength and fracture toughness of a given composite material. The double cantilever beam test with moment loading was found to be a sensitive test under mode I cracking to characterise interphase differences mechanically. The crack initiation values relate directly to differences in strength measurements. The parameters of the bridging laws differ significantly for the four composite systems. Implementation of these laws into ABAQUS visualises the significant differences in R-curve behaviour and crack opening shapes.

ACKNOWLEDGEMENTS

The authors would like to thank the Danish Polymer Centre, the Materials Research Department at Risø and LM Glasfiber A/S (Torben K. Jacobsen) for their support with the project.

References

1. **Rice**, **J. R.** "A path independent integral and the approximate analysis of strain concentration by notches and cracks", *J. Appl. Mech.*, **35** (1968), 379-386.
2. **Sørensen**, **B. F.** and **Jacobsen**, **T. K.** "Large-scale bridging in composites: R-curves and bridging laws", *Comp. Part A - Appl. S.*, **29A** (1998), 1443-1451.
3. **Feih, S.**, **Wei, J.**, **Kingshott, P. K.**, and **Sørensen, B. F.** "The influence of fibre sizing on strength and fracture toughness of glass fibre reinforced composites", *Comp. Part A - Appl. S.*, (accepted 2004).
4. **Suo, Z.**, **Bao, G.**, and **Fan, B.** "Delamination R-curve phenomena due to damage", *J. Mech. Phys. Solids*, **40**/1 (1992), 1-16.
5. **Wei, J.**, **Feih, S.**, and **Kingshott, P. K.** (2004) to be submitted.
6. **Jacobsen, T. K.** and **Sørensen, B. F.** "Mode I intra-laminar crack growth in composites – modelling of R-curves measured from bridging laws", *Comp. Part A - Appl. S.*, **32** (2001), 1-11.
7. **Spearing, S. M.** and **Evans, A. G.** "The role of fibre bridging in the delamination resistance of fiber-reinforced composites", *Acta Metall. Mater.*, **40**/9 (1992), 2191-2199.
8. **Lindhagen, J.E.**, **Jekabsons, N.** and **Berglund, L.A.** "Application of bridging-law concepts to short-fibre composites. 4. FEM analysis of notched tensile specimens", *Compos. Sci. Technol.*, **60** (2000), 2895-2901.